JOURNAL OF GEOPHYSICAL RESEARCH, VOL. 101, NO. E2, PAGES 4673–4682, FEBRUARY 25, 1996

Modeling of fluidized ejecta emplacement over digital topography on Venus

Jeffrey R. Johnson[1]

Department of Geosciences, Lunar and Planetary Laboratory, University of Arizona, Tucson

Lisa Gaddis

Branch of Astrogeology, U.S. Geological Survey, Flagstaff, Arizona

Abstract. The FLOW computer model of McEwen and Malin (1989) modified for application to the study of Venus fluidized ejecta blankets (FEBs) demonstrates that relatively low viscosities, yield strengths, and initial velocities are required to duplicate the observed flow paths of the outflow materials. The model calculates the velocities and simulated flow paths of gravity flows over Magellan topography. The model is formulated to determine flow movements from initial conditions, gravitational acceleration, and resistance to motion as described by Coulomb, viscous, and turbulent resistance forces. Successful duplication of observed FEB flow paths has been achieved for the FEB craters Addams, Isabella, and Cochran. When used as a simple energy-line model, the model requires low coefficients of friction to extend FEBs to near their observed termini in the synthetic aperture radar (SAR) imagery, although the resulting straight flow lines do not follow the observed flow paths well. For Bingham flow, the model requires low values of viscosity and yield strength which are more similar to pyroclastic or debris flows than basaltic lavas. Flows of 100-m depth require 1 to 2 orders of magnitude higher values of both viscosity and yield strength than 10-m-deep flows. The complicated nature of the flow lines for the low velocity model suggests that FEBs were probably emplaced under variably laminar and turbulent flow conditions, where underlying topography influenced both the direction and energy of flow materials.

Introduction

Among the more intriguing landforms observed in the synthetic aperture radar (SAR) images acquired by the Magellan mapping mission are thin, lobate, radar-bright deposits that appear to originate within the continuous ejecta blanket of many impact craters on Venus and flow for great distances (up to several crater diameters from the crater rim) along topographic gradients [*Phillips et al.*, 1991; *Schaber et al.*, 1992; *Schultz*, 1992b; *Asimow and Wood*, 1992; *Chadwick and Schaber*, 1993; *Johnson and Baker*, 1994]. These "fluidized ejecta blankets" (FEBs) [e.g., *Komatsu et al.*, 1991; *Baker et al.*, 1992] or "outflow deposits" [e.g., *Asimow and Wood*, 1992] often have complicated, fluvial-like morphologies and may include channel systems similar to those discovered in the plains [e.g., *Komatsu et al.*, 1993]. The mechanisms of origin and emplacement of these low-viscosity deposits remain uncertain. They may result from segregation and drainage of impact melted/vaporized materials from within crater ejecta materials via channels [*Baker et al.*, 1992; *Chadwick and Schaber*, 1993], possibly by lava and/or debris flow transport mechanisms [*Asimow and Wood*, 1992; *Johnson and Baker*, 1994] and/or materials fluidized by interaction of the expanding ejecta curtain with the dense Venusian atmosphere [*Schultz*, 1992a, 1992b]. In general, the FEB material is believed to have been generated instantly during the impact event and to consist of mixed impact melt and debris [*Chadwick and Schaber*, 1993; *Johnson and Baker*, 1994; *Ivanov et al.*, 1992].

Details of FEB rheologies can help determine whether the outflow deposits are more consistent with lava flowlike or debris flowlike behaviors. Preliminary efforts to determine the rheologies of the outflow materials have concentrated on subjective measurements of channel levee widths using simple Bingham plastic flow models [*Asimow and Wood*, 1992; *Schaber et al.*, 1992]. We use a numerical flow model to define flow paths and velocities for FEBs using topographic data derived from the Magellan altimeter. Agreement between predicted and observed flow distributions enables us to constrain rheologic parameters and possibly material and chemical composition for the FEB materials.

Background and Methodology

Computer simulation of flow emplacement processes have been used to study terrestrial and planetary lava flows [e.g., *Wadge et al.*, 1994; *Bruno et al.*, 1994; *Hanley and Zimbelman*, 1995; *Zimbelman and Hanley*, 1995], pyroclastic flows, lahars, avalanches [*McEwen and Malin*, 1989; *Woods and Bursik*, 1994], and Martian fluidized ejecta blankets [*Ivanov et al.*, 1994]. *McEwen and Malin* [1989] presented the FLOW computer model to calculate velocities and simulated flow paths of gravity flows over digital elevation models (DEMs) for several types of gravity flows that occurred at Mt. St. Helens (MSH) in May 1980. The model was

[1]Now at Planetary Geosciences, University of Hawaii, Honolulu

Paper number 95JE02361.
0148-0227/95/95JE-02361/$05.00

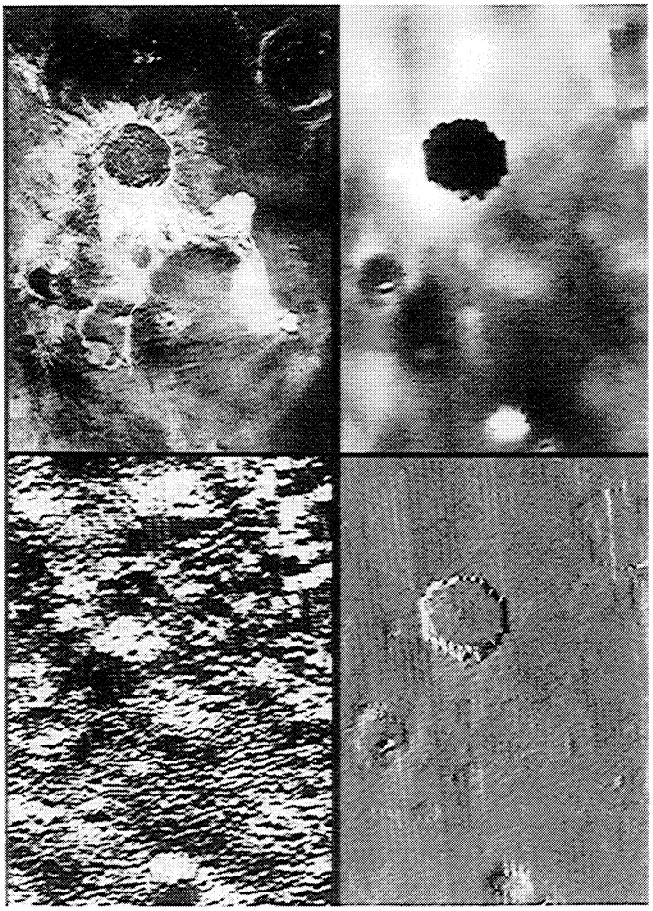

Figure 1. Isabella crater SAR image (upper left), GTDR topography image (upper right), azimuth image (lower left), and slope (dip) image (lower right) computed from GTDR image using GRADE16 program. In the slope image, white pixels are the steepest east-dipping slopes, while black pixels are the steepest west-dipping slopes. In the azimuth image, slopes oriented to the north are bright, while slopes to the south are dark (see text). Also note that some commercially available software packages may also provide similar slope and slope azimuth information for a given DEM [cf. *Hanley and Zimbelman*, 1995].

formulated to determine flow movements from initial conditions, gravitational acceleration, and resistance to motion (τ_r) as described by the generalized equation

$$\tau_r = (a_0 + a_1 v + a_2 v^2) \quad (1)$$

where v is velocity and the terms a_0, a_1, and a_2 are empirically related to Coulomb, viscous, and turbulent resistance, respectively. An energy-line model [*Hsü*, 1975; *Sheridan*, 1979] was used by relating a_0 to a coefficient of friction and setting a_1 and a_2 to zero, although it often predicted flow velocities that were higher than those observed during the MSH events and thus not significantly affected by the DEM topography. A Bingham flowlike model using the a_1 and a_2 terms resulted in more consistent flow velocities and directions, especially when the effects of flow turbulence were incorporated in the model.

In cooperation with A. McEwen (U.S. Geological Survey, Flagstaff), the FLOW model has been modified slightly for application to the study of Venus FEB impact crater flows. (This modification mainly involves changing the gravitational constant to 8.81 m/s^2, and expanding the output parameters to account for higher velocities and flow lengths than those encountered for the MSH model runs). Renamed VFLOW, the model is used in combination with Venus DEMs constructed from the global topographic data records (GTDR) collected by the Magellan altimeter [cf. *Saunders et al.*, 1992; *Ford and Pettengill*, 1992].

Slope (dip) and slope azimuth images are first constructed from the topography images using the GRADE16 program (also written by McEwen). This algorithm uses the spatial and vertical resolution of the input DEM and trigonometric relations between adjacent pixels to calculate data number (DN) values that are proportional to the magnitude of the local topographic slope and to the azimuth of that slope. Slope images are initially calculated in which DN values of 126 correspond to flat surfaces, while DN values of 1 correspond to a 90° dip toward the western hemisphere, and DN values of 251 correspond to a 90° dip toward the eastern hemisphere. Once the magnitude and sign (i.e., east versus west) of the dip have been calculated, the slope azimuth is obtained. If the slope (as determined in the slope image) is eastward (westward), a DN value of 91 corresponds to an exactly eastern (western) azimuthal slope direction. In both cases, a DN value of 1 corresponds to a southern slope azimuth, while a DN value of 181 corresponds to a northern slope azimuth. Thus the combination of the slope and slope azimuth images is required to uniquely determine the three-dimensional orientation of a particular DEM element. Figure 1 shows an example of SAR, topography, slope, and azimuth images for the crater Isabella.

The output from VFLOW consists of two images of the flow lines with DN values proportional to velocity and time along each flow line. Since we are more interested in the derived flow paths, the output flow lines are transformed into white lines that are overlain on the SAR images (Figures 2-4). Flow lines end where the cross-sectional velocity of the flow is zero. A summary of the resistance parameters and the equations of motion is presented below.

Results for the VFLOW model for the FEB craters Addams, Isabella, and Cochran are then presented, followed by a discussion of the implications of the results. These three FEB craters were chosen to provide a range of topographic settings and because of previous studies of their radar properties [e.g., *Johnson and Baker*, 1994]. Addams (90-km diameter) is located on the eastern edge of a corona-chain complex in northeastern Lada Terra. The 600-km-long FEB flow follows the shallow (~0.002) eastward dipping slope along its length, with distal ponding in depressions. Isabella (175 km) is located in a plains region north of Imdr Regio between two large corona complexes. The complicated, channelized FEB branches into southern and eastern lobes, subject to preexisting topographic obstacles (e.g., domes, large rises). Slopes along flow are shallow (~0.002) but variable [cf. *Johnson and Baker*, 1994]. Cochran (100 km) is located in the plains southeast of Ananke Tessera [cf. *Schaber et al.*, 1992]. The northwestern portion of the FEB has flowed into the highland tessera and been deflected into a southeast trending flow, which travels along very shallow (< 0.001) slopes for over 200 km.

Note that direct observations of flow velocities aided modeling of the MSH events. Without such observations, the results presented here using VFLOW are intended primarily to

Table 1. VFLOW Model Results for Addams, Isabella, and Cochran

Model	v_o, m/s	k, Pa	tan ϕ	η, Pa s	c_g	D, m	dD/dt, m/s	Re/Bi	Figure
				Addams (R=45,000 m)					
ADD1	230	--	0.0065	--	--	--	--	--	
ADD2	230	15	--	40	--	10	--	1,319	
ADD3	230	900	--	3,000	--	100	--	1,495	2a
ADD4	230	900	--	3,000	0.01	100	--	1,495	
ADD5	230	900	--	1,500	--	100	0.015	1,136	
ADD6	100	--	0.0015	--	--	--	--	--	
ADD7	100	100	--	5	--	10	--	487,537	
ADD8	100	5	--	25	--	10	--	1,199	2b
ADD9	100	300	--	1,900	--	100	--	1,245	2c
ADD10	100	8	--	200	--	100	0.015	28	2d
				Isabella (R=87,500 m)					
ISA1	321	--	0.014	--	--	--	--	--	
ISA2	321	30	--	60	--	10	--	1,236	
ISA3	321	2,500	--	5,000	--	100	--	1,494	3a
ISA4	321	2,700	--	3,200	--	100	0.015	1,879	
ISA5a	100	--	<0.001	--	--	--	--	--	
ISA5b	100	--	0.003	--	--	--	--	--	
ISA6a	100	10	--	35	--	10	--	1,218	3b
ISA6b	100	5	--	20	--	10	--	1,835	3c
ISA7a	100	400	--	2,300	--	100	--	1,128	
ISA7b	100	200	--	1,400	--	100	--	1,517	3d
ISA8a	100	200	--	900	--	100	0.015	1,677	
ISA8b	100	65	--	225	--	100	0.015	25	
				Cochran (R= 50,000 m)					
CO1	242	--	0.04	--	--	--	--	--	
CO2	100	--	0.01	--	--	--	--	--	
CO3	100	55	--	80	--	10	--	1,288	4a
CO4	100	2,700	--	5,800	--	100	--	1,202	4b
CO5	100	200	--	2,000	--	100	--	749	4c
CO6	100	2,700	--	5,800	--	100	0.015	1,153	
CO7	10	2	--	10	--	10	--	2,934	4d

v_o = initial flow velocity, k = yield strength, tan ϕ = coefficient of friction, η = viscosity, c_g = drag coefficient, D = flow depth, dD/dt = deposition rate, Re/Bi = Reynolds number/Bingham number ratio, R = crater radius

provide some constraints on the rheological properties of the FEB flow materials and their ability to travel long distances over nearly flat terrain.

VFLOW Model Parameters

VFLOW is designed to compute three-dimensional flow paths over DEMs by using nonuniform flow models (i.e., those in which the flow acceleration or deceleration varies, depending on the surface slope angle) in which the flow direction and velocity are recomputed at each time step. The acceleration of a columnar element of flow is given by

$$dv/dt = g\sin\theta - (a_0 + a_1 v + a_2 v^2) / \rho D \quad (2)$$

where t is time, g is the acceleration of gravity, θ is the slope of the ground (from the slope image computed from the DEM), ρ is the density of the flow material, and D is the depth of the flow. The VFLOW model assumes that (1) the flow depth stays approximately constant or linearly decreases with time; and

Table 2a. VFLOW Model Results for 10-m Flow Depths

Model	v_o, m/s	k, Pa	η, Pa s	Figure
ADD2	230	15	40	
ADD8	100	5	25	2b
ISA2	321	30	60	
ISA6a	100	10	35	3b
ISA6b	100	5	20	3c
CO3	100	55	80	4a

Table 2b. VFLOW Model Results for 100-m Flow Depths

Model	v_o, m/s	k, Pa	η, Pa s	Figure
ADD3	230	900	3000	2a
ADD9	100	300	1900	2c
ISA3	321	2500	5000	3a
ISA7a	100	400	2300	
ISA7b	100	200	1400	3d
CO4	100	2700	5800	4b
CO5	100	200	2000	4c

Table 2c. VFLOW Model Results for 100-m Flow Depths and Deposition Rate of 0.015 m/s

Model	v_o, m/s	k, Pa	η, Pa s	Figure
ADD5	230	900	1500	
ADD10	100	8	200	2d
ISA4	321	2700	3200	
ISA8a	100	200	900	
ISA8b	100	65	225	
CO6	100	2700	5800	

(2) the flow is approximately steady state, i.e., changes in the mass flux of the flow materials are not considered. Where these assumptions are valid, the VFLOW model parameters may be related to rheological properties of the flow materials such as yield strength and viscosity.

The Coulomb resistance parameter a_0 represents a constant force per unit area, independent of flow velocity, as described by

$$\tau_r = C + \sigma \tan\phi \quad (3)$$

where C is the cohesion, σ is the normal stress ($Mg\cos\theta$, where M is the mass of the flow), and ϕ is the angle of internal friction. If cohesion is ignored, this model is equivalent to an "energy-line" or "grain-flow" model, in which the friction coefficient, $\tan\phi$, can be represented by the ratio of the total vertical drop (H) to the total horizontal travel distance (L) of the flow [e.g., *Lowe*, 1976; *Sheridan*, 1979]. Although lacking rigorous empirical or theoretical justification, the energy-line model was a useful empirical model for the MSH work of *McEwen and Malin* [1989] when used in conjunction with velocity-dependent (viscous or turbulent) resistance terms, and is also used here.

The viscous resistance term a_1 is characterized by a Bingham rheology, where

$$\tau_r = k + \eta(dv/dy) \quad (4)$$

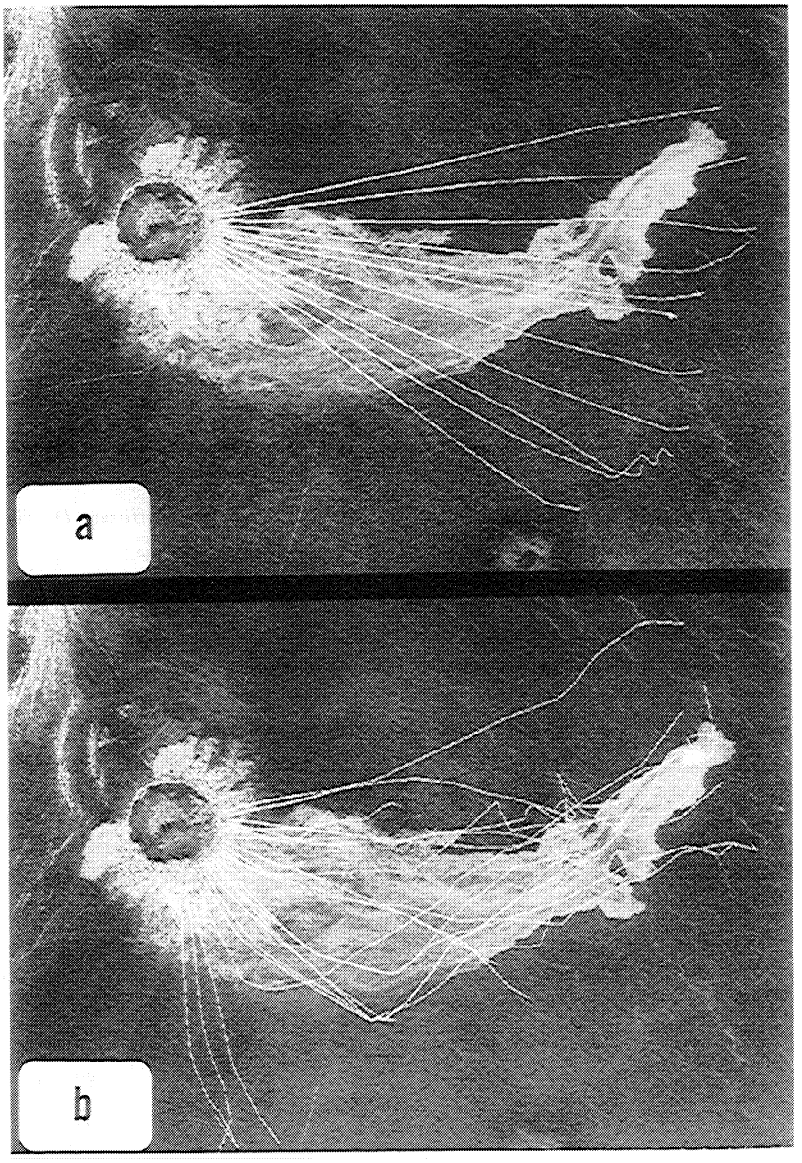

Figure 2. Flow lines from VFLOW runs superimposed on SAR image of Addams for runs (a) ADD3 (high initial velocity), (b) ADD8 (10-m flow depth, low velocity), (c) ADD9 (100-m flow depth, low velocity), and (d) ADD10 (includes deposition rate of 0.015 m/s).

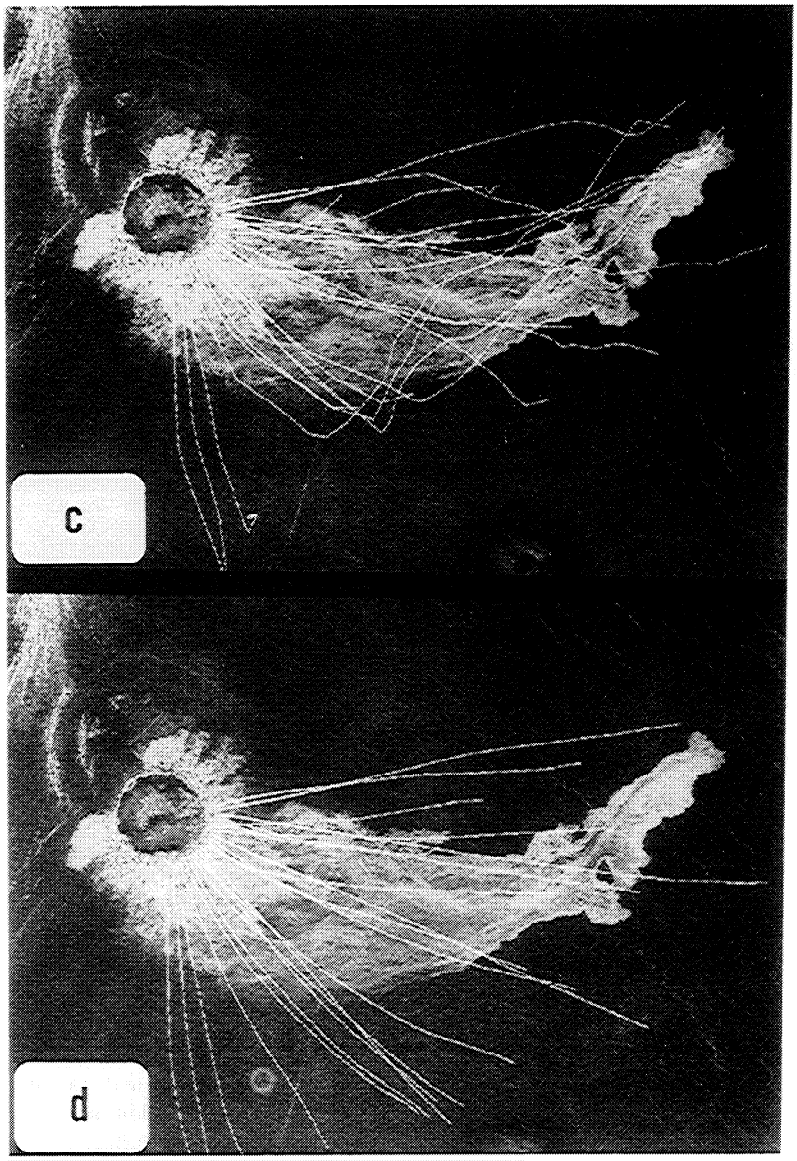

Figure 2. (continued)

where k is the yield strength in Pascals (Pa) and includes both cohesion and frictional strength, η is viscosity (in Pa s), and y is the distance below the surface of the flowing material such that dv/dy is the velocity gradient or shear strain rate in laminar flow. *Johnson* [1970] derived the velocity gradient for a Bingham flow, including the effects of the central, rigid "plug" that develops in the center and top of a channelized flow where the gravitational stress does not exceed the yield strength. The acceleration of the plug in a wide channel (assumed for the FEBs) is given by FLOW as

$$dv_p/dt = g\sin\theta - [(2k) / (\rho(D + D_c)] - [(2\eta v_p) / \rho(D^2 - D_c^2)] \quad (5)$$

where v_p is the velocity of the plug and D_c is the diameter of the plug. The mean cross-sectional velocity (v) of a Bingham flow in a wide channel is then given by FLOW as

$$v = (1/D)\int_{D_c}^{D} v(y)dy + v_p D_c/D \quad (6)$$

where $v(y)$ is the velocity profile for steady, uniform flow in a wide channel given by

$$v(y) = (1/\eta)\ \{[\rho g\sin\theta(D^2 - y^2)/2] - k\,(D - y)\} \qquad (y \geq Dc) \quad (7)$$

In the FLOW model, v_p is first computed substituting v_o (the initial flow velocity) for v_p in (5). Then v_p is substituted for $v(y)$ in (6) before integration to calculate the flow velocity.

In FLOW, turbulent resistance (a_2 in (2)) is divided into two components: (1) turbulent shear against the flow surface; and (2) atmospheric resistance along the surface of the flow. Turbulent resistance against the ground is estimated by use of the Chezy equation:

$$\tau_r = 0.5 c_g \rho v^2 \quad (8)$$

with a drag coefficient (c_g) taken here as 0.01 [*McEwen and Malin*, 1989]. Atmospheric resistance was neglected in FLOW for dense flows (1000-2000 kg/m^3), although it could be significant for lower-density flows, especially in the denser atmosphere of Venus. This effect has not been included in the current version of VFLOW, however.

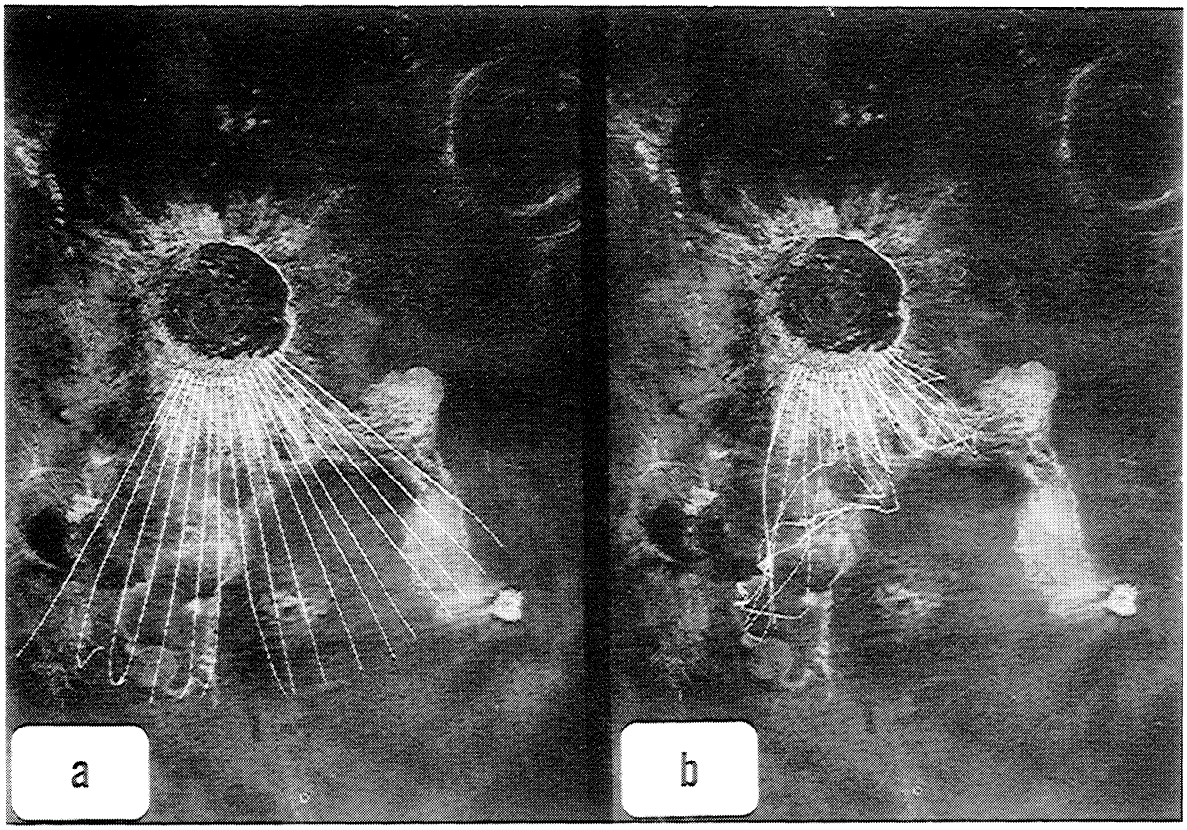

Figure 3. Flow lines from VFLOW runs superimposed on SAR image of Isabella for runs (a) ISA3 (high initial velocity), (b) ISA6a (10-m flow depth, low velocity, best fit for western/central FEB), (c) ISA6b (10-m flow depth, low velocity, best fit for the eastern FEB lobe), and (d) ISA7b (100-m flow depth, low velocity, best fit for the eastern FEB lobe).

Transition from laminar to turbulent Bingham flow occurs when the ratio of the Reynolds number (Re) to Bingham number (Bi) is greater than about 1000, where

$$Re = \rho v D/\eta \quad (9)$$

$$Bi = kD/\eta v \quad (10)$$

The emplacement of FEB flows likely occurs in a proximal turbulent regime, followed distally by more laminar flow, although transitions between the flow styles may be complicated [*Chadwick and Schaber,* 1993; *Johnson and Baker,* 1994]. In the results presented below, VFLOW model runs attempt to keep the Re/Bi ratio slightly greater than 1000 to account for existence of the two flow regimes.

Results

McEwen and Malin [1989] used the original FLOW model in two ways: as an energy-line model (in which the coefficient of friction is the only resisting force) and as a Bingham flow model (in which yield strength and viscosity, as well as drag forces, are included). The same approach has been taken here using VFLOW. Table 1 shows the results of 29 model runs, while Tables 2a-2c simplify the results for particular run sets. The Isabella "a" runs correspond to qualitatively determined best fits for the central and western FEB regions, while the "b" runs are for the main eastern lobe. Blank spaces in Table 1 represent values that were not used or not calculated in the model run.

It should be recognized that the DEMs used here contain artifacts such as inter-orbit variations (e.g., the "striped" appearance of Figure 1) that may influence the flow paths to an uncertain extent. In addition, an inherent assumption is that the current state of the surface topography is the same as when the FEB was emplaced. This may not be the case for some regions, such as the 20-km-diameter crater Cohn, which is superimposed on the Isabella main FEB flow lobe. As such, qualitative matches of the flow lines to the observed FEBs are expected more often than exact replication of the FEB paths.

While some model parameters used by *McEwen and Malin* [1989] were available from measurements of the MSH flows, the flows here are not constrained by such measurements. Initial ejection velocities are calculated using the method of *Ivanov et al.* [1994]:

$$v_o = (2/15*gR)^{1/2} \quad (11)$$

which is similar to the initial velocity given by *Melosh* [1989] from energy-scaling theory:

$$v_o = 0.28(r/R)^{-1.8}(gD)^{1/2} \quad (12)$$

where r (the position within the crater) is equal to R (the crater radius) and D is the crater diameter. A series of runs using these initial velocities are followed by runs in which the velocity is arbitrarily set to 100 m/s (Table 1). Preliminary runs showed that higher density flows usually resulted in longer flows and lower densities in shorter flows, but for simplicity, flow density is kept at a constant 1500 kg/m^3 in the runs presented here [cf. *McEwen and Malin,* 1989]. Flow

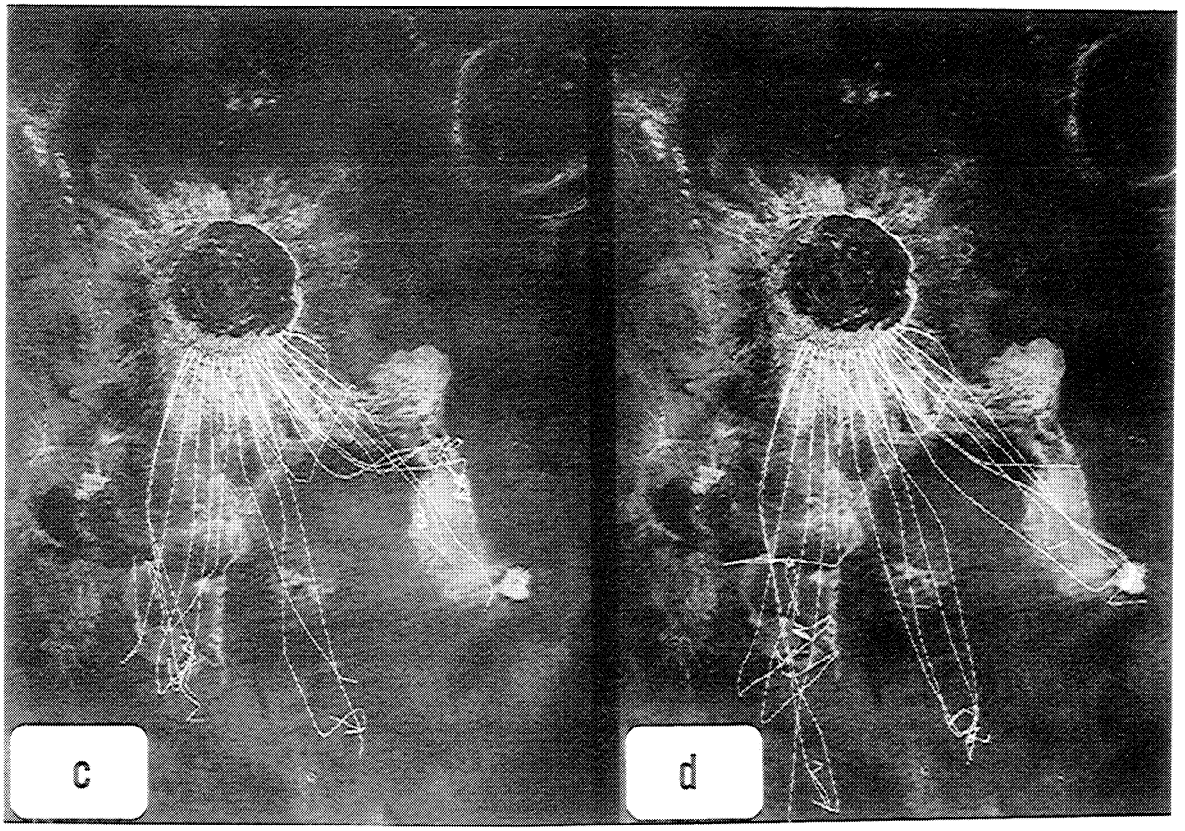

Figure 3. (continued)

depths are chosen as 10 m and 100 m [cf. *Phillips et al.*, 1991; *Schultz*, 1992b].

All runs for which a calculated initial velocity is used (ADD1-ADD5, ISA1-ISA4, CO1) result in very straight flow lines that do not follow the FEB paths very well and exhibit only minor distal responses to topography (e.g., ADD3 in Figure 2a and ISA3 in Figure 3a). Flows at 100 m/s initial velocity respond to topography better and follow the observed FEB flows moderately well (e.g., ADD8 in Figure 2b). Inclusion of a drag coefficient of 0.01 does not alter the flow paths or the resistance parameters greatly for any of the FEBs (e.g., ADD4).

The energy-line model was run for each crater under two different initial velocities (model runs ADD1, ADD6, ISA1, ISA5, CO1, and CO2). The coefficient of friction values (tan ϕ) required to extend the flow lines to the end of the observed FEB flows vary from < 0.001 to 0.04, with Cochran showing the highest values. These values are quite low compared to terrestrial pyroclastic flows and avalanches, which usually have values between 0.1 and 0.2 [e.g., *McEwen and Malin*, 1989], although the volcanic debris avalanche at Nevado de Colima in Mexico exhibits a value 0.04 [*Stoopes and Sheridan*, 1992], and some ignimbrites may show values < 0.02 [*Fisher and Schmincke*, 1984, p. 227]. One of the lowest terrestrial values observed is that for the submarine Saharan debris flow deposit on the northwest African continental margin, which traveled some 700 km over greater than 2 km of relief, resulting in a coefficient of friction of ~0.003 [*Masson et al.*, 1993]. For comparison, *Hawke and Whitford-Stark* [1982] found that the Chenier crater impact melt flows on the Moon showed a coefficient of friction of 0.073.

Table 3. Yield Strength and Viscosity of Some Terrestrial and Venusian Flow Materials

Material	Yield strength, Pa	Viscosity, Pa s	Reference
Mauna Loa lavas	66-1,898	100-100,000	*Moore* (1987)
Basaltic lavas	50-250,000	200-230,000	*Pinkerton and Wilson* (1994)
Kilauea lavas	5000-50,000	5×10^5-8×10^6	*Fink and Zimbelman* (1986)
MSH pyroclastics, etc.	500-600	4-4,700	*McEwen and Malin* (1989)
MSH avalanche	10,000	30,000	*McEwen and Malin* (1989)
Carbonatites/komatiites	?	< 1.0	*Kargel et al.* (1995)
Black Canyon debris flow	80-2,150	18-430	*Whipple and Dunne* (1992)
Venus FEBs	24-6,100	0.28-100,000	*Asimow and Wood* (1992)
Isabella FEB	200-2,600 Pa	--	*Schaber et al.*,(1992)

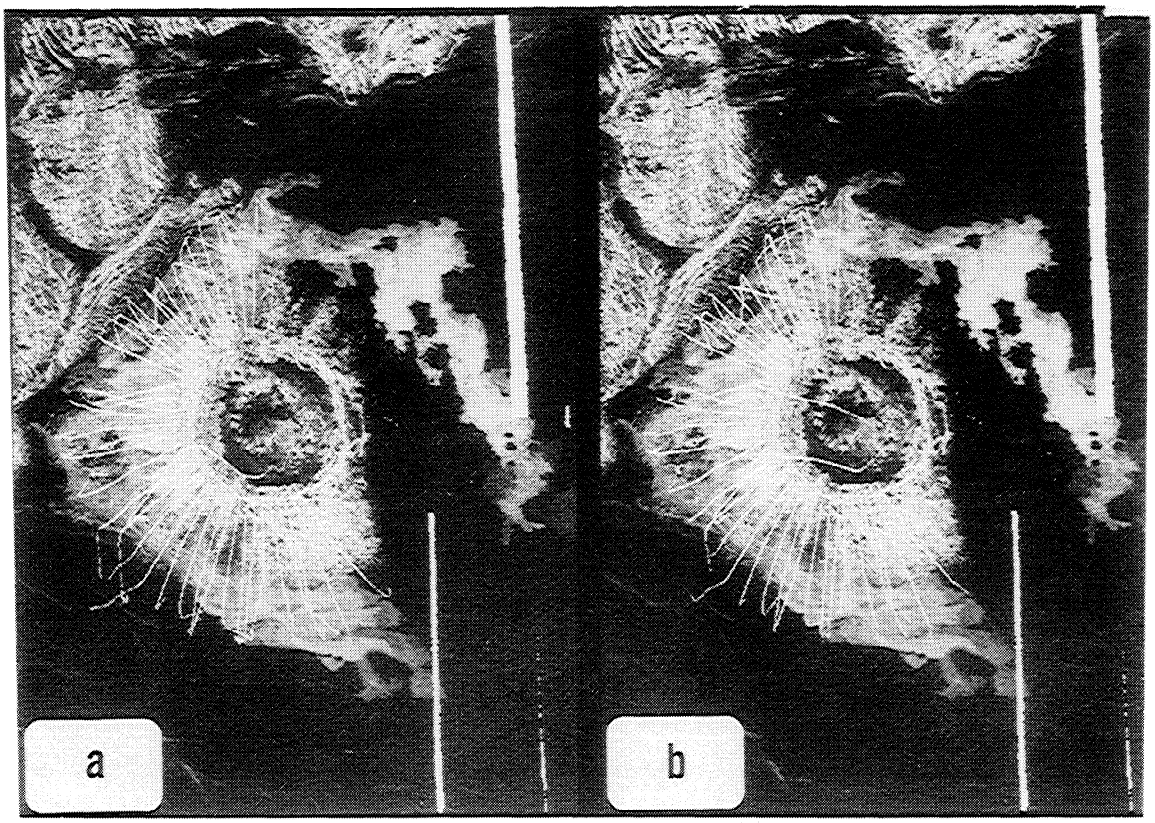

Figure 4. Flow lines from VFLOW runs superimposed on SAR image of Cochran for runs (a) CO3 (10-m flow depth, low velocity, fit for western FEB), (b) CO4 (100-m flow depth, low velocity, fit for western FEB), (c) CO5 (100-m flow depth, low velocity, fit for northern flow lobe extent), and (d) CO7 (10-m flow depth, lowest velocity (10 m/s), fit for northern flow lobe extent).

For the Bingham models, flow depths of 10 m require yield strengths from 5 to 55 Pa, and viscosities from 20 to 80 Pa s (Table 2a), with the 100 m/s initial velocity runs requiring lower values of both. These values are relatively low in comparison to terrestrial basaltic lavas and more like some debris flows (Table 3). Also, exotic lavas such as carbonatites and komatiites have lower viscosities (<1.0 Pa s; Table 3) and have been proposed as possible components of the FEB flows [*Baker et al.*, 1992; *Kargel et al.*, 1994]. Although the low yield strengths for 10-m flow depths are somewhat anomalous, attempts to model the FEBs using higher yield strengths at the expense of lower viscosities result in undesirably high *Re/Bi* values, as in run ADD7 (Table 1).

Flow depths of 100 m require yield strengths from 200 to 2700 Pa and viscosities from 1400 to 5800 Pa s (Table 2b). These values are somewhat more like those of basaltic lavas, but still as low as some pyroclastic and debris flow values. Other workers have estimated similar to somewhat larger values for Venus FEB flows (Table 3). Morphologic study of the FEBs has suggested that flow depths are probably of the order of 10 m, especially distally where blocking of the flows by low-relief features is often seen [e.g., *Schultz*, 1992b].

VFLOW includes an option to decrease the flow depth by a constant amount each time step. This "deposition rate" is chosen as 0.015 m/s for runs shown in Table 2c. This factor lowers the required values of yield strength and viscosity to 8-2700 Pa and 200-5800 Pa s. The effect is minimal for Cochran, the shortest flow, and is difficult to model for the other flows with respect to achieving an appropriate *Re/Bi* value. Slight changes to the input parameters result in either very low or very high *Re/Bi* values, suggesting that a flow with linearly decreasing depth is more prone to changes between laminar and turbulent regimes.

The southeastern portions of the Cochran flow are particularly difficult to model because of the change in direction of the flow to an easterly flow after encountering the northern highland tessera. In run CO5 (Figure 4c; Table 2b) use of a lower yield strength (200 Pa) and viscosity (2000 Pa s) than run CO4 results in one flow line that follows the northern FEB lobe rather well, although other lines extend too far. This suggests that a lower initial velocity might provide a better match to the FEB path. Run CO7 shows the result of a 10 m/s velocity, which requires very low values of yield strength (2 Pa) and viscosity (10 Pa s) to provide two flow lines that follow the northern FEB lobe very well. Other lines again extend too far, or are trapped within the crater itself due to the irregular nature of the boundaries of the crater in the low-resolution topography data. Also, the *Re/Bi* value is somewhat high (2934), but can be lowered by decreasing the yield strength and/or viscosity further. These runs suggest that the FEB flows for Cochran may have traveled as low-velocity (<10 m/s), low yield strength flows with low viscosity in order to account for the observed emplacement geometry.

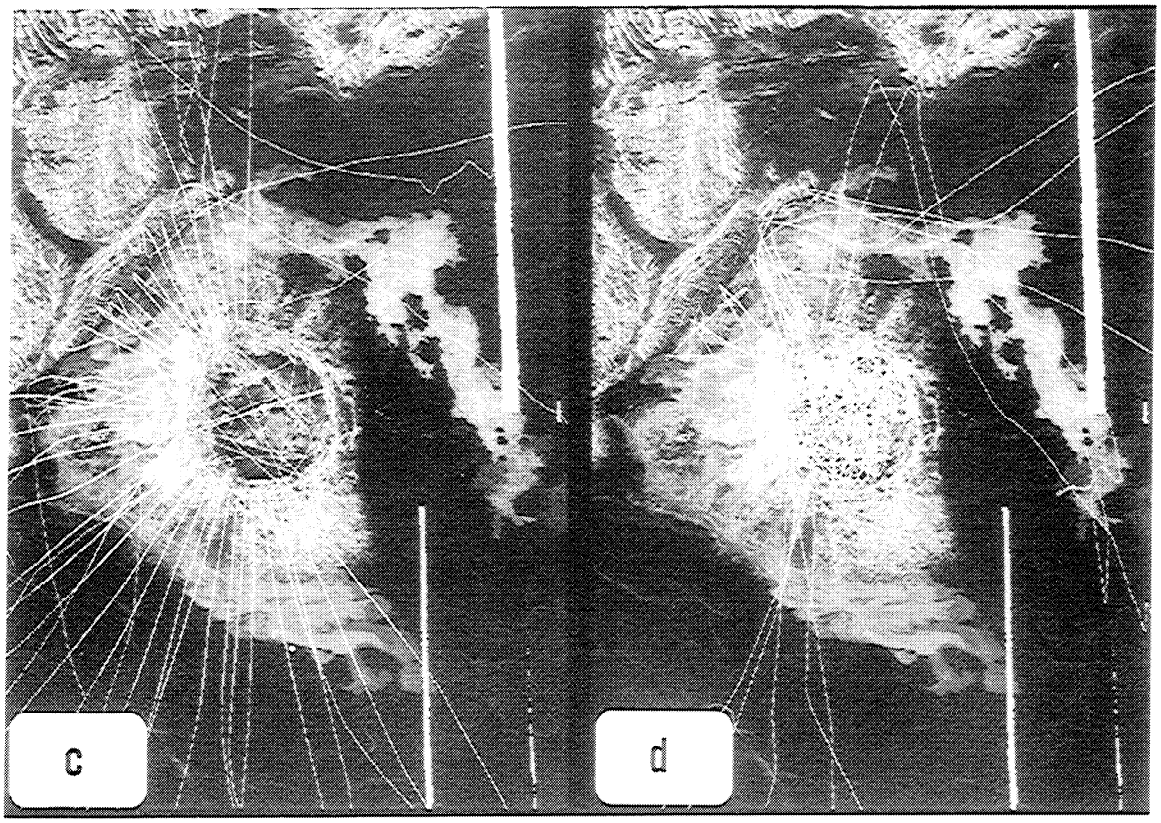

Figure 4. (continued)

Discussion and Summary

The results for the three FEB craters presented above provide important, although not unambiguous, information regarding the emplacement processes and rheology of the FEB flow materials. The following generalizations and constraints on FEB flow processes can be made based on the current VFLOW runs.

Application of the energy-line model to these FEBs results in very low coefficient of friction values, similar to the lowest values observed for some terrestrial pyroclastic and avalanche materials, or the large submarine debris flows off the coast of Africa [*Fisher and Schmincke*, 1984; *Masson et al.*, 1993]. A more realistic approach is to model the FEB flows as Bingham materials. This results in yield strength and viscosity values that are much lower than those for basaltic lavas and more similar to pyroclastic or debris flows or more unusual lava types (e.g., carbonatites [*Kargel et al.*, 1994]), depending on the given FEB flow depth and initial velocity (Tables 2 and 3).

The choice of initial velocity is very important to appropriately model the FEB flow path. Initial impact ejection velocities calculated using (11) are too large and result in flow lines that do not respond well to topography, as shown in Figures 2a and 3a. Velocities of 100 m/s allow the flow lines to model better the flow paths (e.g., Figures 2b and 3b), although at the expense of requiring lower resistance parameter values (Table 1). The case of Cochran is especially insightful in this regard. The longest FEB flow paths of this crater cannot be modeled well using an initial velocity of 100 m/s (Figure 4c). Only when the velocity is decreased to 10 m/s can these flow lobes be approximately modeled, and only then by using correspondingly lower resistance parameters (Figure 4d, Table 1).

VFLOW runs with 10-m- or 100-m-deep flows can equally well mimic FEB flow paths (compare Figures 2b with 2c, Figures 3c and 3d, or Figures 4a and 4b). However, the 100-m flows require higher values of both resistance parameters than 10-m-deep flows (Tables 2a and 2b). Morphologic evidence suggests, however, that 100-m-flows may be rarer, especially distally [*Phillips et al.*, 1991; *Schultz*, 1992b]. Although ambiguities in flow thickness estimates remain, it appears that the VFLOW model will provide acceptable results for flow depths between 10 and 100 m.

Incorporation of a deposition rate in the VFLOW runs may more realistically portray FEB emplacement. These runs require slightly lower resistance parameters, but experience greater difficulty in maintaining Re/Bi values near the turbulent/laminar transition. Additionally, flow paths cannot be as accurately modeled using the deposition rate parameter (e.g., Figure 2d).

The complicated overlapping and intersecting nature of flow lines resulting from the VFLOW models emphasizes that the FEBs were probably emplaced under conditions where transitions between laminar and turbulent flow occurred often, especially at lower velocities, where the effects of the underlying topography would influence both the direction and energy of the flow materials. Thus FEB emplacement appears not to involve a simple, singular rheologic style, at least at the scale of these large FEB craters. Rather, complicated

changes in flow style more readily explain the observed flow paths. Such transitions are consistent with results obtained from studies of radar property variations along FEBs [*Johnson and Baker*, 1994].

Thus the modeling described here is consistent with FEBs emplaced as intermediate to low velocity, 10- to 100-m-deep flows with low frictional resistance and/or with very low yield strengths and viscosities, similar to some terrestrial debris or pyroclastic flows, or possibly very low viscosity lavas. Importantly, transitions between flow styles due to variable flow velocities and responses to topography result in complicated, overlapping morphologies that cannot be attributed to a single flow rheology.

Future work with VFLOW will include other FEB craters in different topographic settings. Also, since increasing the density of the flows from the constant 1500 kg/m^3 used here resulted in longer flows, future runs with higher densities should require higher resistance parameter values (more like those in Table 3) to model the FEBs. Atmospheric drag should also be incorporated into VFLOW in order to determine the resistance effect of the 60 kg/m^3 Venusian atmosphere. Finally, better DEMs would allow more accurate modeling of the FEB flow paths using VFLOW. This may be possible for some regions using multiple-cycle SAR stereo images [e.g., *Leberl et al.*, 1992], where complete coverage exists for each cycle.

Acknowledgments: This work was supported through NASA Magellan JPL contract 958493, by NASA Venus Data Analysis Program grant NAGW-3515, and by Planetary Geology and Geophysics grant NAGW-285. Helpful formal reviews of this work were provided by Nadine Barlow and Jim Zimbelman, and an informal review by Goro Komatsu. The assistance of Alfred McEwen with the FLOW code is greatly appreciated. Thanks for software/hardware support to the Planetary Image Research Laboratory (University of Arizona) including R. Singer, B. Castalia, J. Winburn, J. Plassman, and A. Papanikolas.

References

Asimow, P.D., and J.A. Wood, Fluid outflows from Venus impact craters: Analysis from Magellan data, *J. Geophys. Res.*, *97*, 13,643-13,665, 1992.

Baker, V.R., G. Komatsu, T.J. Parker, V.C. Gulick, J.S. Kargel, and J.S. Lewis, Channels and valleys on Venus: Preliminary analysis of Magellan data, *J. Geophys. Res.*, *97*, 13,421-13,444, 1992.

Bruno, B.C., S.M. Baloga, G.J. Taylor, and M.J Tatsumura, Lava flow rheology: A comparison of data and theory (abstract), *Lunar Planet. Sci. Conf., XXV*, 189-190, 1994.

Chadwick, D.J., and G.G. Schaber, Impact crater outflows on Venus: Morphology and emplacement mechanisms, *J. Geophys. Res.*, *98*, 20,891-20,902, 1993.

Fink, J.H., and J.R. Zimbelman, Rheology of the 1983 Royal Gardens basalt flows, Kilauea Volcano, Hawaii, *Bull. Volcanol.*, *48*, 87-96, 1986.

Fisher, R.V., and H.-U. Schmincke, *Pyroclastic Rocks*, 472 pp., Springer-Verlag, New York, 1984.

Ford, P.G., and G.H. Pettengill, Venus topography and kilometer-scale slopes, *J. Geophys. Res.*, *97*, 13,103-13,114, 1992.

Hanley, D., and J.R. Zimbelman, Topographic control of lava flow emplacement: Earth, Mars, and Venus (abstract), *Lunar Planet. Sci. Conf., XXVI*, 545-546, 1995.

Hawke, B.R., and J. Whitford-Stark, The Chenier crater flows: Evidence for an origin as Tsiolkovsky impact melt (abstract), *Lunar Planet. Sci. Conf., XIII*, 310-311, 1982.

Hsü, K.J., Catastrophic debris streams (Sturzstroms) generated by rockfalls, *Geol. Soc. Am. Bull.*, *86*, 129-140, 1975.

Ivanov, B.A., I.V. Nemchinov, V.A. Svetsov, A.A. Provalov, and V.M. Khazins, Impact cratering on Venus: Physical and mechanical models, *J. Geophys. Res.*, *97*, 16,167-16,181, 1992.

Ivanov, B.A., B.C. Murray, and A.S. Yen, Dynamics of fluidized ejecta blankets on Mars (abstract), *Lunar Planet. Sci., XXV*, 599-600, 1994.

Johnson, A.M., *Physical Processes in Geology*, chaps. 12-14, Freeman, Cooper, San Francisco, Calif., 1970.

Johnson, J.R., and V.R. Baker, Surface property variations in Venusian fluidized ejecta blanket craters, *Icarus*, *110*, 33-70, 1994.

Kargel, J.S., B. Fegley, A. Treiman, and R.L. Kirk, Carbonate-sulfate volcanism on Venus?, *Icarus*, *112*, 219-252, 1994.

Komatsu, G., J.S. Kargel, V.R. Baker, J.S. Lewis, and R.G. Strom, Fluidized impact ejecta and associated impact melt channels on Venus (abstract), *Lunar Planet. Sci., XXII*, 741-742, 1991.

Komatsu, G., V.R. Baker, V.C. Gulick, and T.J. Parker, Venusian channels and valleys: Distribution and volcanological implications, *Icarus*, *102*, 1-25, 1993.

Leberl, F.W., J.K. Thomas, and K.E. Maurice, Initial results from the Magellan stereo experiment, *J. Geophys. Res.*, *97*, 13,675-13,689, 1992.

Lowe, D.R., Grain flow and grain flow deposits, *J. Sediment. Petrol.*, *46*, 188-199, 1976.

Masson, D.G., Q.J. Huggett, and D. Drunsden, The surface texture of the Saharan debris flow deposit and some speculations on submarine debris flow processes, *Sedimentology*, *40*, 583-598, 1993.

McEwen, A.S., and M.C. Malin, Dynamics of Mount St. Helens' 1980 pyroclastic flows, rockslide-avalanche, lahars, and blast, *J. Volcanol. Geotherm. Res.*, *37*, 205-231, 1989.

Melosh, H.J., *Impact Cratering: A Geologic Process*, 245 pp., Oxford University Press, New York, 1989.

Moore, H.J., Preliminary estimates of the rheological properties of 1984 Mauna Loa lava, *U.S. Geol. Surv. Prof. Pap.*, *1350*, 1569-1588, 1987.

Phillips, R.J., R.E. Arvidson, J.M. Boyce, D.B. Campbell, J.E. Guest, G.G. Schaber, and L.A. Soderblom, Impact craters on Venus: Initial analysis from Magellan, *Science*, *252*, 288-297, 1991.

Pinkerton, H., and L. Wilson, Factors controlling the lengths of channel-fed lava flows, *Bull. Volcanol. 56*, 108-120, 1994.

Saunders, R. S., et al., Magellan mission summary, *J. Geophys. Res.*, *97*, 13,067-13,090, 1992.

Schaber, G.G., R.G. Strom, H.J. Moore, L.A. Soderblom, R.L. Kirk, D.J. Chadwick, D.D. Dawson, L.R. Gaddis, J.M. Boyce, and J. Russell, Geology and distribution of impact on Venus: What are they telling us?, *J. Geophys. Res.*, *97*, 13,257-13,301, 1992.

Schultz, P.H., Atmospheric effects on ejecta emplacement, *J. Geophys. Res.*, *97*, 11,623-11,662, 1992a.

Schultz, P. H., Atmospheric effects on ejecta emplacement and crater formation on Venus from Magellan, *J. Geophys. Res.*, *97*, 16,183-16,248, 1992b.

Sheridan, M.F., Emplacement of pyroclastic flows: A review, *Spec. Pap., Geol. Soc. Am.*, *180*, 125-136, 1979.

Stoopes, G.R., and M.F. Sheridan, Giant debris avalanches from the Colima Volcanic Complex, Mexico: Implications for long-runout landslides (>100 km) and hazard assessment, *Geology*, *20*, 299-302, 1992.

Wadge, G., P.A.V. Young, and I.J. McKendrick, Mapping lava flow hazards using computer simulation, *J. Geophys. Res.*, *99*, 489-504, 1994.

Whipple, K.X., and T. Dunne, The influence of debris flow rheology on fan morphology, Owens Valley, California, *Geol. Soc. Amer. Bull.*, *104*, 887-900, 1992.

Woods, A.W., and M.I. Bursik, A laboratory study of ash flows, *J. Geophys. Res.*, *99*, 4375-4394, 1994.

Zimbelman, J.R., and D. Hanley, Topographic control of lava flow emplacement on Venus and Mars (abstract), *Eos, Trans. AGU, Spring Meet. Suppl.*,*76*(17), S191, 1995.

L. Gaddis, U.S. Geological Survey, Branch of Astrogeology, 2255 N. Gemini Road, Flagstaff, AZ 86001. (e-mail: lgaddis@iflag2.wr.usgs.gov)

J.R. Johnson, Planetary Geosciences, University of Hawaii, 2525 Correa Road, Honolulu, HI 96822. (e-mail: jjohnson@kahana.pgd.hawaii.edu)

(Received March 4, 1995; revised July 31, 1995; accepted August 1, 1995.)